Volume 16
Number 38
14 October 2025
Pages 17509–17972

Chemical Science

rsc.li/chemical-science

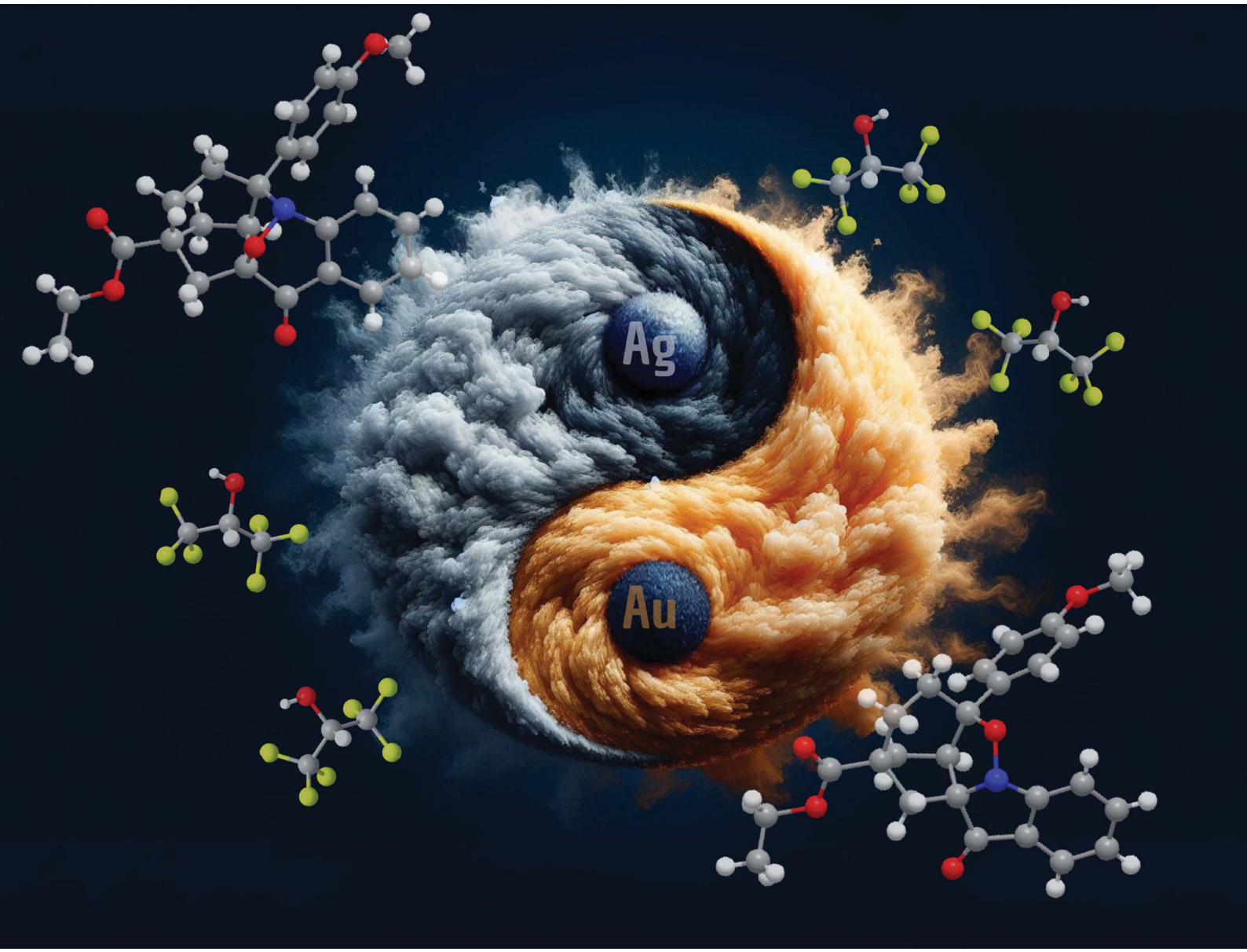

ISSN 2041-6539

EDGE ARTICLE

Véronique Michelet *et al.*

Silver- and gold-catalyzed divergent cascade cycloisomerization/[3 + 2] *versus* [2 + 2 + 1] cycloaddition towards a stereoselective access to heterohexacyclic derivatives

ROYAL SOCIETY OF CHEMISTRY

15 YEARS ANNIVERSARY

Chemical Science

ROYAL SOCIETY OF CHEMISTRY

EDGE ARTICLE

View Article Online
View Journal | View Issue

Cite this: *Chem. Sci.*, 2025, **16**, 17611

All publication charges for this article have been paid for by the Royal Society of Chemistry

Silver- and gold-catalyzed divergent cascade cycloisomerization/[3 + 2] *versus* [2 + 2 + 1] cycloaddition towards a stereoselective access to heterohexacyclic derivatives

Emilie Gentilini,[a] Anaïs Bouschon,[a] Vincent Davenel,[b] Fabien Fontaine-Vive,[a] Jean-Marie Fourquez[b] and Véronique Michelet *[a]

A divergent cascade cycloisomerization/[3 + 2] *vs.* [2 + 2 + 1]-cycloaddition *via* gold or silver catalysis has been reported in 1,1,1,3,3,3-hexafluoroisopropan-2-ol (HFIP). The reaction was independently optimized for both metals leading to two hexacyclic derivatives comprising a bicyclo[3.2.1]octane unit and respectively a benzoxazinone or a *N*-oxo-indolinone pattern. The unique influence of HFIP was demonstrated *via* ^{19}F and ^{31}P NMR analyses. This process, involving the formation of C–C, C–O, and C–N bonds and of three stereogenic centers led to privileged scaffolds in a context of the search for increased molecular diversity of drug-candidate libraries. The versatility of this methodology was demonstrated by the synthesis of 25 different hexacyclic scaffolds (yields up to 98%). Gram-scale synthesis as well as post-functionalization reactions illustrated the versatility and interest of these catalytic transformations. DFT calculations were performed to rationalize the proposed mechanism of this cascade reaction.

Received 17th July 2025
Accepted 9th September 2025

DOI: 10.1039/d5sc05338b

rsc.li/chemical-science

Introduction

Regarding the relevance of complex heterocycles in biologically active molecules but also the recent concept of "Escape from Flatland",[1] designing new and sustainable methods for access to poly-heterocyclic derivatives appears to be still very challenging. In this context, catalytic cascade cycloisomerization processes offer an access to diverse and complex scaffolds, while maintaining atom economy and mild reaction conditions. Among these cascade reactions, the cycloisomerization of *o*-(alkynyl)nitrobenzene derivatives drew our attention, as in recent years, in addition to the classic reactivity leading to the anthranil or isatogen units,[2] different intra-[3] or intermolecular[4] metal-catalyzed cascade reactions have been reported (Fig. 1). In 2011, Liu and co-workers reported a gold-catalyzed intermolecular nitroalkyne redox cyclization/[2 + 2 + 1]-cycloaddition leading to an azacyclic compound in a stereoselective manner (Fig. 1A).[5] In comparison with the literature on these gold-catalyzed transformations, studies on the catalytic activity of silver compounds are relatively scarce.[6] For example, a sequential silver-catalyzed oxidative cyclization of 2-alkynylanilines has been reported by Arcadi and our group leading to anthranil derivatives (Fig. 1B).[7] Hexafluoroisopropanol (HFIP) is a powerful solvent widely used for stabilizing charged intermediates,[8] but more recently used in organometallic chemistry, particularly in gold catalysis.[9] Its strong hydrogen-bonding ability and high polarity was a key feature for accelerating reaction rates and improving selectivity. The combination of 1,1,1,3,3,3-hexafluoroisopropanol (HFIP) with gold complexes has proven highly effective in catalytic cycloisomerization reactions leading to heterocycles (Fig. 1C).[9]

While combination of HFIP with silver catalysts in cycloisomerization reactions is limited,[10] the synergistic effects observed in gold catalysis suggest that exploring HFIP's role in silver-catalyzed processes could be a promising area for future research. Following our interest in organometallic atom-economical transformations,[11] we therefore embarked in this study and anticipated that this synergy would facilitate the activation of alkynes in the case of silver complexes as for gold catalysts. Additionally, HFIP is known to improve the solubility of substrates and to create a network closed to water network, which would be an asset and would hopefully contribute to high regio- and stereoselectivity in the resulting products.[12]

On the other hand, designing methods for selectively synthesizing different products from the same starting material, only by modifying the reaction conditions and/or the catalysts, is challenging but represents also a valuable tool for divergent synthesis.[13] In this context, starting from a 1,6-cyclohexenylalkyne scaffold, we envisaged to explore the reactivity of

[a]*Université Côte d'Azur, Institut de Chimie de Nice, Valrose Park, 06108, Nice Cedex 2, France. E-mail: veronique.michelet@univ-cotedazur.fr*

[b]*Institut Servier d'Innovation Thérapeutique Paris-Saclay, 22 Route 128 – Rue Francis Perrin, 91190 Gif sur Yvette, France*

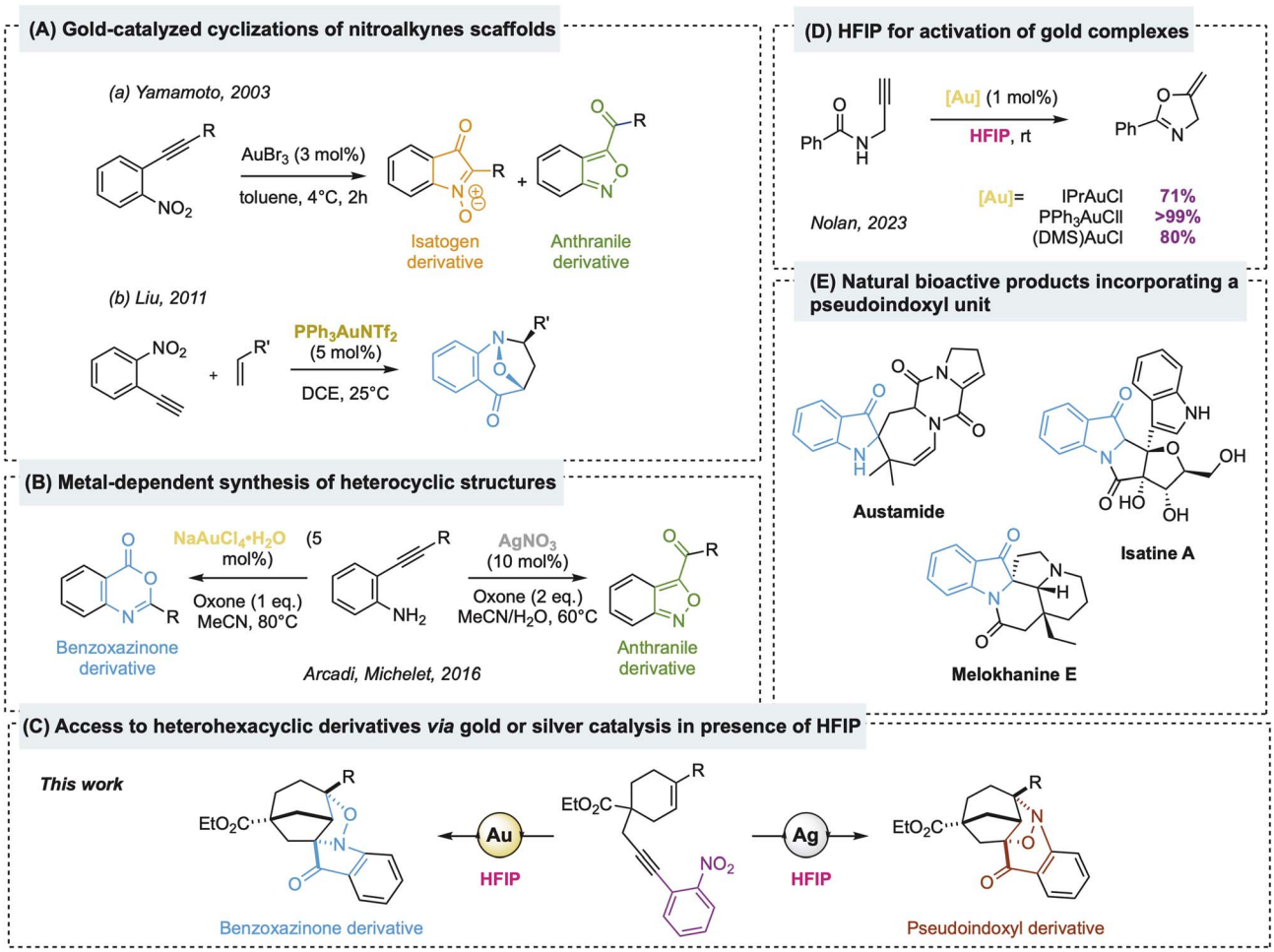

Fig. 1 (A) Gold-catalyzed cyclizations of nitroalkyne scaffolds. (B) Metal-dependent synthesis of heterocyclic structures. (C) Access to heterohexacyclic derivatives *via* gold or silver catalysis in the presence of HFIP. (D) HFIP for activation of gold complexes. (E) Natural bioactive products incorporating a pseudoindoxyl unit.

such substrates while adding an *o*-nitrophenyl on the alkyne (Fig. 1D). Considering the potent reactivity of nitroalkynes derivatives but also of 1,6-enynes, we expected an intramolecular cascade reaction involving these three functions. We wish therefore to report therein a divergent synthesis of two hexacyclic derivatives *via* a silver or gold-catalyzed cycloisomerization and [3 + 2] or [2 + 2 + 1] cycloaddition cascade reaction (Fig. 1D).

Starting from the same compound, and by switching from gold to silver catalysts, we designed two unprecedented selective methods leading to complex scaffolds bearing respectively a benzoxazinone and a *N*-oxo-indolinone units. These structures represent privileged scaffolds in a search for increased molecular diversity of drug-candidate libraries.

Results and discussion

The 1,6-enyne derivatives were prepared through a four-step sequence starting from ethyl 4-oxocyclohexane carboxylate **1**.[11a,14] After triflation, a Suzuki–Miyaura coupling was performed (yields from 64% to 98%) to reach derivatives **3a** to **3i** (Scheme 1). The substrate **3j** was obtained *via* an iron-coupling using MeMgBr and 10 mol% of $Fe(acac)_3$ in a THF/NMP mixture, according to a procedure described by Fürstner's group.[15] Derivatives **3a** to **3j** were then engaged in a propargylation reaction with yields from 28% to 94% and subsequently in a Sonogashira cross-coupling, leading to the desired starting 1,6-enynes **5a** to **5z** (26 derivatives) with yields ranging from 46% to 98% (Scheme 1). The substitution on the aromatic ring R^2 was highly diversified with electron-withdrawing and electron-donating groups. Similar modifications were designed for group R^1 (see SI for details). We also introduced relevant heterocycles such as an indole (**5i**), a nitroquinoline (**5v**) and 2-nitrothiophenes (**5w**, **5x**). We then initiated our study with 1,6-enyne **5b** bearing a *para*-methoxyphenyl as model substrate.

Regarding the different functions, five products were initially observed, bicyclic derivatives **6** and **7** coming from respectively the 6-*endo* and 5-*exo* cycloisomerization of the enyne moiety, product **8b** obtained after the classical nitroalkyne cyclization[15,16] and hexacycles **9b** and **10b** resulting from the cycloisomerization/[3 + 2] or [2 + 2 + 1]-cycloaddition cascade reaction (Table 1).

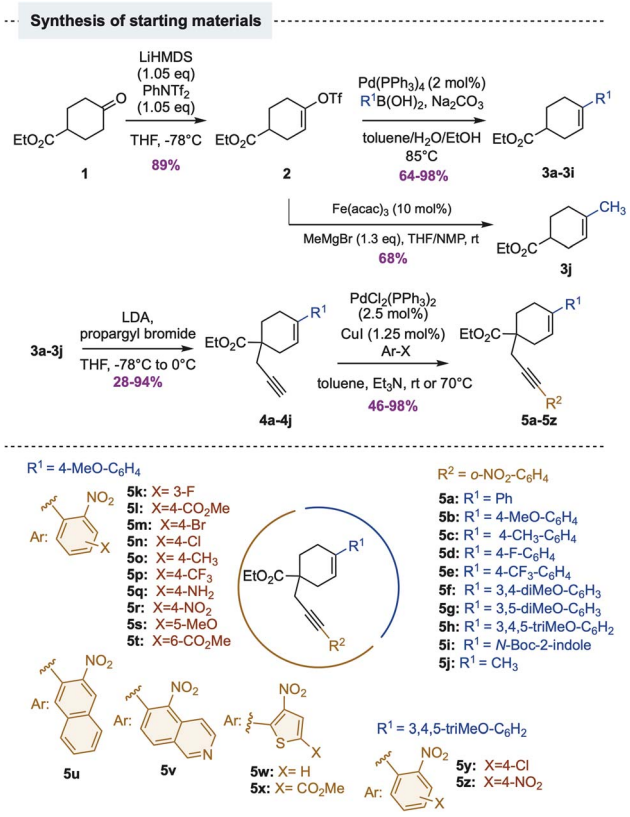

Scheme 1 Synthesis of starting materials.

Regarding the complexity and the similarity of these two products **9b** and **10b**, their structures were unambiguously confirmed by X-ray diffraction of derivatives **9b** and **10b**, bearing a *para*-methoxyphenyl as aromatic ring (Fig. 2).[17]

Due to the similarities between each product, we evaluated ratios between the five products by ^{1}H NMR using 3,4,5-trichloropyridine as an internal standard. We evaluated the efficiency of our previous conditions, eg 5 mol% of $IPrAuNTf_2$ in toluene at 80 °C. We obtained a selectivity of 37% for the anthranile derivative **8b**. We therefore started our investigations by testing different solvents and observed that the use of DCE at room temperature gave a better yield for **8b** (49%) and **10b** (26%) (Table 1, entry 2). We then explored the impact of the ligand. Switching from NHC ligand to PPh_3 provided a major selectivity (56%) for hexacycle **10b**. Keeping in mind the existing literature cited before on the difference of selectivity between the use of silver and gold catalysts on similar transformations,[7] we wondered if silver catalysts were suitable in our reaction. We first employed $AgNO_3$ but unfortunately, no conversion was observed (Table 1, entry 4). Rewardingly, using 5 mol% of $AgNTf_2$ in DCE at room temperature led to the formation of product **9b** as major product despite a modest yield and a partial conversion (Table 1, entry 5). Increasing the temperature to 80 °C allowed a total conversion with a better yield of 55% for **9b** (Table 1, entry 6). Different silver salts had been tested such as $AgSbF_6$, AgOTf, Ag_2CO_3 (Table 1, entries 7 to 9), but none of them gave satisfying results. Interestingly, the use of $AgBF_4$ led to a total selectivity for hexacycle **9b** with a yield of 56% (Table 1, entry 10). Further optimizations in different solvents did not give satisfactory results, as no reaction occurred in toluene or acetonitrile (Table 1, entries 11–12) and a mixture of **8b** and **9b** was observed in nitromethane (Table 1, entry 13). We performed the cyclization in HFIP and observed a better yield of 67% (Table 1, entry 14). To determine if this result was solely due to the protic nature of HFIP or to its properties,[8] we also conducted the reaction in MeOH, ^{i}PrOH, ^{t}BuOH and TFE, but no reactivity was detected (Table 1, entries 15–18). Considering the unstable aspect of silver salts, we envisaged to use a ligand to increase the efficiency of the reaction, unfortunately the addition of 20 mol% PPh_3 resulted in a total loss of reactivity (Table 1, entry 19).[18] Finally, increasing the catalytic charge from 5 to 10 mol% (Table 1, entry 20) allowed to reach a yield of 78%, giving us our final conditions for the formation of **9b**: 10 mol% of $AgBF_4$ in HFIP at 40 °C.

With these successful conditions for **9b** in hands, we then came back to some optimization that would allow the formation of hexacycle **10b**. The best result obtained so far was 43% yield using 5 mol% of PPh_3AuNTf_2 in DCE at room temperature (Table 2, entry 1). We started the optimization by performing the reaction in different solvents, but once again, no better results were obtained in nitromethane, acetonitrile, chloroform or methanol (Table 2, entries 2 to 6). We mentioned earlier the growing interest on the use of HFIP for transition-metal catalysis and this applies particularly to reactions involving gold complexes. HFIP demonstrated indeed an ability to activate gold chloride species. It has been shown that the acidic properties of HFIP weaken the Au–Cl bond by creating a network of hydrogen bonds, enabling the generation of the active cationic gold form.[9] Regarding the drawbacks of the use of additives such as silver salts but also the great solubility of [AuCl(L)] complexes in this solvent, HFIP appeared to be very suitable for methodologies involving gold catalysis. In this context, we performed the reaction in HFIP, using first the active species PPh_3AuNTf_2 which led to a yield of 48% for **10b** (Table 2, entry 7). Switching to the usually unreactive chloride form, PPh_3AuCl, gladly provided a full selectivity for **10b** with a yield of 56% (Table 2, entry 8). We already observed at the beginning of the optimization that NHC ligands favored the formation of **8b**, so the chloride forms of such complexes (IPrAuCl and SIPrAuCl) were also engaged in HFIP (Table 2, entries 8 and 9). A slight difference was observed and a yield of 50% was obtained for **8b** using SIPrAuCl in HFIP at rt (entry 10). Considering the higher ease of use of this catalyst, these conditions were kept as final ones in order to target the anthranile scaffold of product **8**.

Concerning the access to hexacyclic scaffold **10b**, we then explored the effect of other phosphine ligands. We selected two phosphine-based ligands and one phosphite. JohnPhos and the phosphite-ligand based complex (Table 2, entries 11 and 13) gave similar results, a mixture of all the five products with a slight selectivity around 30% for **10b** (with a conversion of 84% for the phosphite) while dppm (Table 2, entry 12) provided a selectivity of 40% for the desired hexacycle. With the best result with triphenylphosphine gold(I) chloride in hand, we finally investigated the effect of the temperature (Table 2,

Table 1 Optimization of reaction targeting hexacycle **9b**

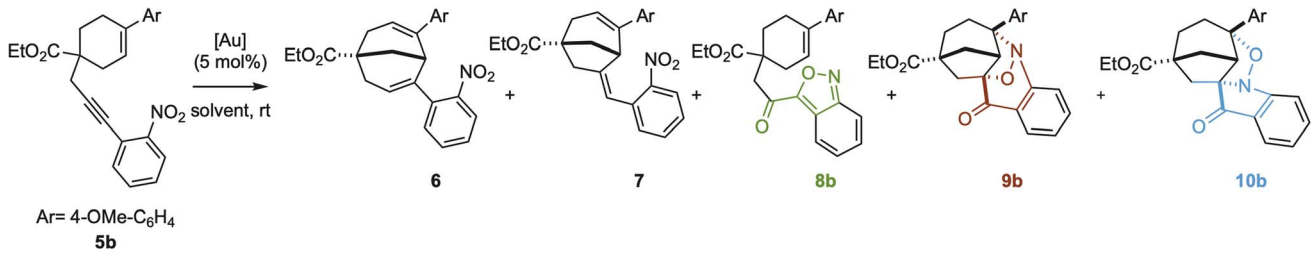

Entry	[M]	T (°C)	Solvent	**6**[a](%)	**7**[a](%)	**8b**[a](%)	**9b**[a](%)	**10b**[a](%)
1	$IPrAuNTf_2$	80	Toluene	4	5	37	Traces	13
2	$IPrAuNTf_2$	rt	DCE	—	—	49	3	26
3	PPh_3AuNTf_2	rt	DCE	3	3	6	21	43
4[b]	$AgNO_3$	rt	DCE	—	—	—	—	—
5[c]	$AgNTf_2$	rt	DCE	—	—	6	31	12
6	$AgNTf_2$	80	DCE	—	—	8	55	—
7	$AgSbF_6$	80	DCE	—	—	—	37	—
8[d]	AgOTf	80	DCE	—	—	—	43	—
9[b]	Ag_2CO_3	80	DCE	—	—	—	—	—
10	$AgBF_4$	80	DCE	—	—	—	56	—
11	$AgBF_4$	80	Toluene	—	—	—	—	—
12[b]	$AgBF_4$	80	MeCN	—	—	—	—	—
13[b]	$AgBF_4$	80	$MeNO_2$	—	—	19	27	—
14	$AgBF_4$	40	HFIP	—	—	—	67	—
15[b]	$AgBF_4$	40	MeOH	—	—	—	—	—
16[b]	$AgBF_4$	40	^{i}PrOH	—	—	—	—	—
17[b]	$AgBF_4$	40	^{t}BuOH	—	—	—	—	—
18[b]	$AgBF_4$	40	TFE	—	—	—	—	—
19[b,e]	$AgBF_4$	40	HFIP	—	—	—	—	—
20[f]	$AgBF_4$	40	HFIP	—	—	—	78	—
21[f]	$AgBF_4$	80	DCE	—	—	—	65	—
22[g]	—	80	DCE	—	—	—	—	—

[a] Determined by ^{1}H NMR. [b] 0% conversion. [c] 66% conversion. [d] 62% conversion. [e] Addition of 20% of PPh_3. [f] 10 mol% of [Ag]. [g] Addition of 10 mol% of $HNTf_2$, only degradation of starting material was observed.

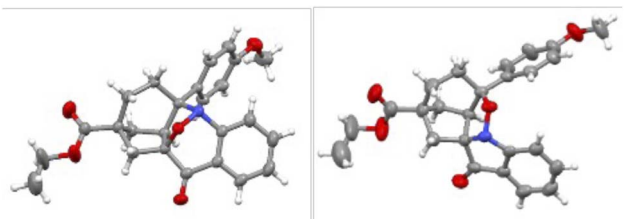

Fig. 2 X-ray diffractions of **9b** (left) and **10b** (right).

entries 14 and 15) but we observed lower activity at lower or higher temperature. A control experiment without gold species was performed and no reaction was observed (Table 2, entry 16). Thus, we finally chose as final conditions for **10b** the use of 5 mol% of PPh_3AuCl in HFIP at room temperature.

Interactions between metal complexes and HFIP had also been investigated *via* NMR studies: with ^{19}F NMR for $AgBF_4$ (Fig. 3, left) and ^{31}P NMR for PPh_3AuCl (Fig. 3, right).

Both signals (in green) showed an upfield signal in presence of HFIP compared to the one of the complexes alone (in red). This result supports the existence of an interaction between the complex used — either gold or silver — and HFIP, potentially leading to the formation of a network between these species. This could also explain the particular selectivity observed when HFIP is used as the solvent.

With selective conditions for each of the desired products in hand, we then started to evaluate the scope and the limitations of our reactions, by first targeting hexacycle **9b** bearing a bicyclo [3.2.1]octane and a benzoxazinone units (Scheme 2).

We began by the modification of the R^1 group. Our model substrate was with a *p*-methoxy-phenyl, so we first ran the reaction with a phenyl substituent that led to the exact same yield of 78% (**9a**, **9b**). Switching to *p*-tolyl (**9c**) or 3,4-dimethoxyphenyl (**9f**) aromatic rings provided the desired compound in modest yields. Unfortunately, we could not isolate product **9d**, where R^1 was a *p*-fluorophenyl group. The synthesis of starting materials bearing electron-withdrawing groups on R-position was somewhat complicated, however, the silver-

Table 2 Optimization of reaction targeting hexacycle **10b**

Entry	[M]	Solvent	**6**[a](%)	**7**[a](%)	**8b**[a](%)	**9b**[a](%)	**10b**[a](%)	Conv[b](%)
1	PPh_3AuNTf_2	DCE	2	4	6	21	43	
2	PPh_3AuNTf_2	Toluene	6	6	—	18	41	
3	PPh_3AuNTf_2	$MeNO_2$	2	—	—	16	18	76
4	PPh_3AuNTf_2	MeCN	1	—	5	11	10	69
5	PPh_3AuNTf_2	$CHCl_3$	4	—	—	18	20	90
6	PPh_3AuNTf_2	MeOH	—	—	—	—	—	0
7	PPh_3AuNTf_2	HFIP	—	—	—	4	48	
8	PPh_3AuCl	HFIP	—	—	—	—	56	
9	IPrAuCl	HFIP	—	—	47	7	17	
10	SIPrAuCl	HFIP	—	—	50	6	20	
11	L^1AuCl	HFIP	8	4	14	8	30	
12	$L^2Au_2Cl_2$	HFIP	6	4	6	—	40	
13	$L^3Au_2Cl_2$	HFIP	3	—	9	8	28	84
14[c]	PPh_3AuCl	HFIP	—	—	—	11	36	90
15[d]	PPh_3AuCl	HFIP	—	—	—	—	50	
16	None	HFIP	—	—	—	—	—	0

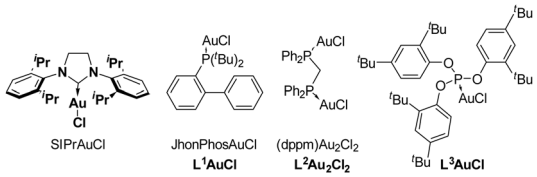

[a] Determined by ^1H NMR. [b] Conversion when not full. [c] Reaction performed at 0 °C. [d] Reaction performed at 40 °C.

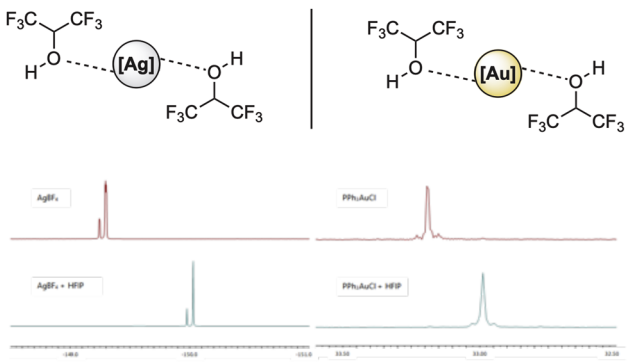

Fig. 3 Interactions of $AgBF_4$ and PPh_3AuCl with HFIP in ^{19}F NMR (left) and ^{31}P NMR (right).

catalyzed cyclization step provided compound **9e** in a good yield of 65%. The *para* position for substitution seemed to be crucial, with no reaction occurring for example with **9g**, while an excellent yield of 98% was obtained for **9h** bearing 3,4,5-trimethoxyphenyl as R^1. We started to perceive the limitation of our catalytic system with *N*-Boc-indole instead of the phenyl group (**9i**). With a methyl group in position R^1, the desired compound **9j** was also not observed, but another product was isolated (Scheme 6, *vide infra*). We continued our investigations by modifying the aromatic ring bearing the nitro group. Adding a fluor in *meta* position led to hexacycle **9k** with a fair yield of 65%. The influence of electronic properties of the aromatic substituent (R^2) was also evaluated: the presence of an electron-donating group led to a loss of reactivity, as no conversion was observed for **5o**, **5q** and **5s**. In contrast, the introduction of electron-withdrawing groups proved to be effective, with yields ranging from 48% to 76%. The steric hindrance was also studied, using methylester in *ortho* (**9t**) and *para* (**9l**) positions as substituents on the R^2 aromatic ring. We obtained the corresponding products with respectively 74% and 76% yields, indicating that the *ortho* position is as well tolerated as the *para*. We were pleased to observe that the reaction conditions were also suitable with halogen substituents (**9m**, **9n**), allowing to envisage cross-couplings as further post-functionalization. The use of larger aromatic systems such as naphthalene provided product **9u**, which could not be cleanly isolated from several by-products. Replacing the phenyl ring by a quinoline one also proved successful, with 50% yield for the compound **9v** while the introduction of a thiophene unit didn't allow the synthesis of hexacyclic compounds **9w** and **9x**. Regarding the excellent yield obtained using 3,4,5-trimethoxyphenyl as R^1 group (**9h**), we wondered if it was compatible with more decorated R^2 aromatic rings. Finally, compounds **9y** and **9z** were isolated with slightly better yields than their respective *p*-methoxyphenyl substituted analogs (72% yield for **9y** compared to 65% for **9n** and 50% yield for **9z** compared to 48% for **9r**).

To investigate the scope of the formation of product **10**, we selected diverse substrates and explored their reactivity using triphenylphosphine gold chloride as catalyst. These conditions appeared unexpectedly to be more challenging compared to those optimized derivative **9** (Scheme 3). Indeed, only seven out of the twelve derivatives led to the desired corresponding

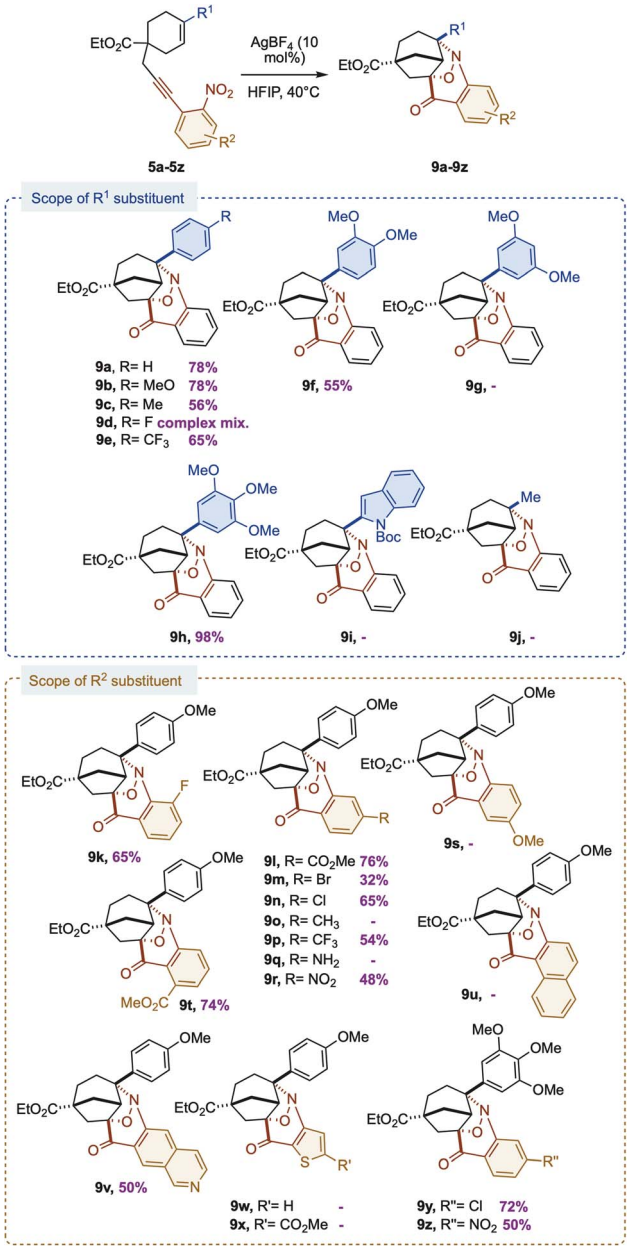

Scheme 2 Scope and limitations of the synthesis of derivatives **9**.

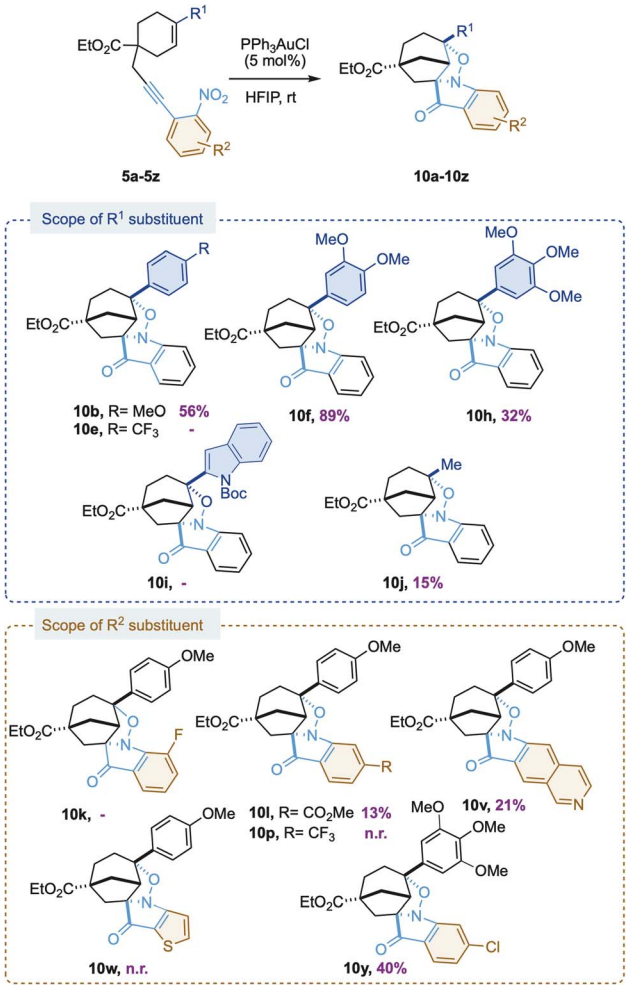

Scheme 3 Scope and limitations of the synthesis of derivatives **10**.

compounds. In the case of **10e** and **10i**, a mixture of starting material and the anthranile derivatives **8**, resulting solely from the cyclization of the nitro moiety with the alkyne, was observed. Rewardingly, we were pleased to observe that switching *p*-methoxyphenyl to 3,4-dimethoxyphenyl as R^1 led to the formation of hexacycle **10f** with 89% yield, and 3,4,5-trimethoxyphenyl provided **10h** with 32% yield. Remarkably, substitution with a methyl group was also suitable with these conditions and led to compound **10j** with a yield of 15%. Concerning R^2 substituent, adding an ester moiety in *para* position decreased the yield to 13% (**10l**) while adding a Cl atom led to a 40% yield (**10y**). Replacing the phenyl by a quinoline ring (**10v**) provided a modest yield of 21%. Example **10k** was, for its part, observed on the crude ^{1}H NMR spectra but unfortunately could not be isolated from several by-products.

To fully complete our study and get a vast array of products, the formation of anthranile scaffold **8** was also investigated, using the conditions described in Table 2, entry 10. Six 1,6-enynes were engaged in presence of 5 mol% of SIPrAuCl in HFIP at room temperature (Scheme 4). Switching from *p*-methoxyphenyl (**8b**, 50% yield) to a phenyl (**8a**) or a 3,5-dimethoxyphenyl (**8c**) allowed the formation of desired compounds with a similar yield of 51%. Concerning R^2, three different positions (C3, C4, C5) and substituents were investigated. The introduction of a fluor atom provided compound **8k** with a yield of 56% while a methoxy in C5-position led to **8s** with a slightly lower yield of 44%. For its part, bromo-substituted anthranile derivative **8m** was obtained with a satisfying yield of 69% (Scheme 4).

Concerning the mechanism of the reaction, different pathways could be envisaged (Schemes 5 and 6). Bicyclo[3.2.1]nonene **6** and bicyclo[3.2.1]octene **7** resulted respectively from the cycloisomerization of the 1,6-enyne moiety under a 6-*endo* or a 5-*exo* pathway, as already described by our group.[11a] Anthranile derivative **8** was obtained by cyclization of the nitroalkyne framework. Such reactivity has been well described in the

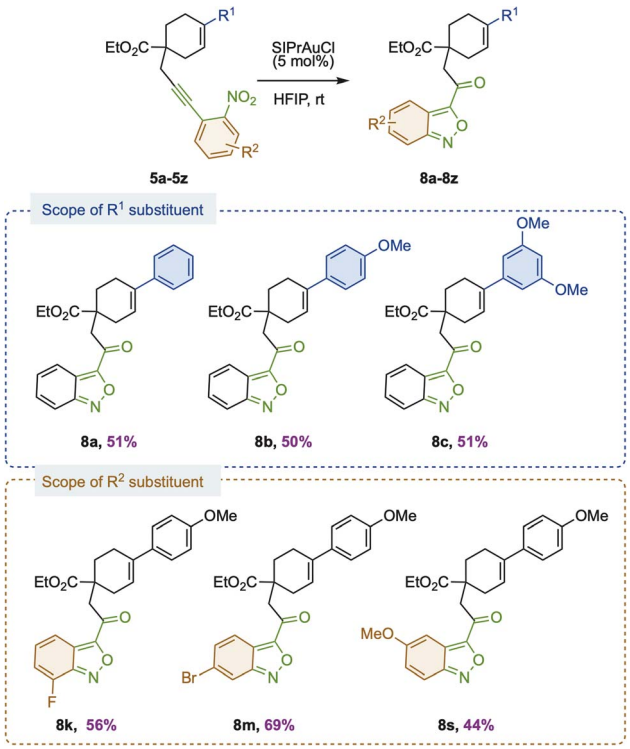

Scheme 4 Scope and limitations of the synthesis of derivatives **8**.

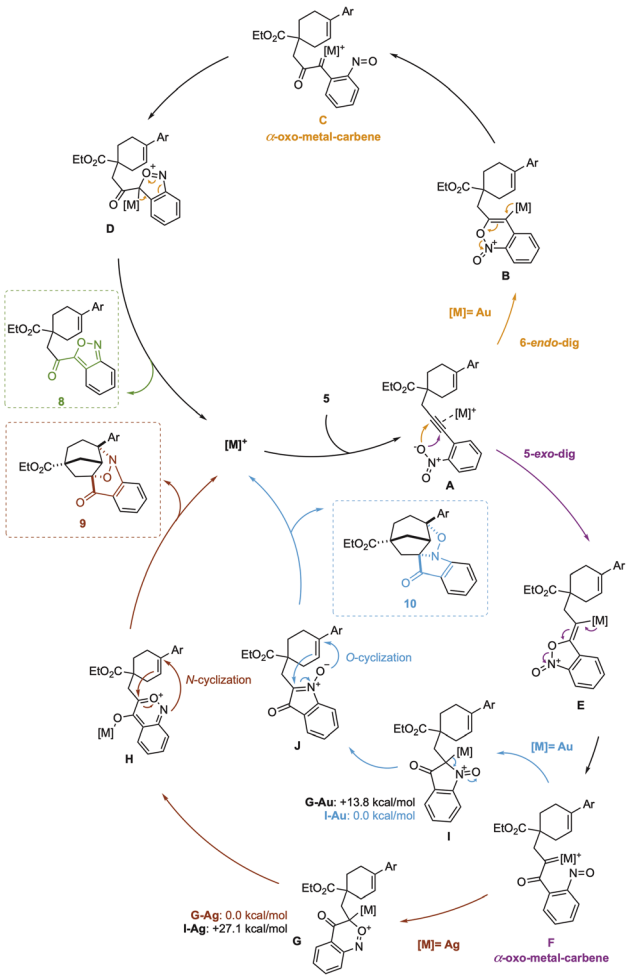

Scheme 5 Proposed mechanism of the reaction.

literature,[3] so we could easily assume that the addition of the nitro group onto the gold-activated alkyne occurred *via* a 6-*endo*-dig process leading to compound **8** *via* the α-oxo-gold-carbene intermediate **C** (Scheme 5). Regarding hexacyclic derivatives **9** and **10**, based on the literature,[3,5] we envisaged that the nitro function could be added *via* a 5-*exo*-dig route allowing the formation of α-oxo-metal-carbene intermediate **F**. The passage through such intermediate had been proven thanks to an intramolecular trapping on substrate **5j** (Scheme 6). Indeed, in presence of $AgBF_4$, the cyclization of **5j** did not lead to the expected hexacyclic derivative **9j** but product **11** was isolated with a yield of 82%. In the presence of PPh_3AuCl, **10j** was synthesized with a yield of 15% but **11** was also obtained as a major product (46% yield).

This product resulted from the intramolecular trapping of intermediate **5j-F** by the alkene of the cyclohexene scaffold (Scheme 6). These results demonstrated the existence of α-oxo-silver-carbene and α-oxo-gold-carbene as intermediates for the synthesis of hexacyclic derivatives **9** and **10**.

Then, two different routes could be proposed for the subsequent intramolecular cyclization of metal carbenoid **F**. Indeed, depending on the heteroatom of the nitroso group involved in the coordination, the α-oxo-metal-carbene **F** could cyclize to form either a five-membered ring with a coordination of the nitrogen, or a six-membered ring with a coordination of the oxygen atom. We investigated *via* DFT calculations the different free energies of these intermediates in the presence of gold and silver complexes in order to rationalize the selectivity between the two metals. Interestingly, in the case of a silver catalyst, the coordination of oxygen, leading to the six-membered ring intermediate **G-Ag** appeared to be the most stable species. Intermediate **I-Ag**, corresponding to nitrogen-coordination had a higher free enthalpy of 27.1 kcal mol^{-1} (Scheme 5, **G-Ag** *vs.* to **I-Ag**).[19] Nevertheless, while using triphenylphosphine gold chloride as catalyst, the formation of the five-membered ring was favored by a difference of 13.8 kcal mol^{-1}.

These results and some data from the literature provide strong support to propose the following mechanism. In the presence of a silver catalyst, the second cyclization occurring is a [2 + 2 + 1] cycloaddition between the alkene, the nitroso moieties and the carbon bearing the gold complex as depicted in Scheme 7.[20] This [2 + 2 + 1] cycloaddition proceeded first by the coordination of the oxygen atom, leading to the six-membered ring **G**. After a keto–enol tautomerism generating enol **H**, a [3 + 2] cycloaddition step would allow the *N*-cyclization to furnish benzoxazinone derivative **9**. In the case of triphenylphosphine gold chloride as catalyst, the coordination of the nitrogen atom of the nitroso would be preferred, leading to pseudoindoxyl scaffold **I** (Scheme 5). We assumed that the demetallation would then occur, leading to the metal-free

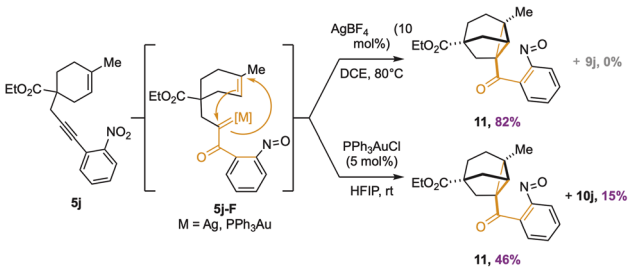

Scheme 6 Intramolecular trapping of α-oxo-metal-carbenes.

nitrone **J**. Finally, the intramolecular [3 + 2] cycloaddition could be performed *via* a *O*-cyclization leading to derivative **10**.

In order to unveil the existence of the potential enol intermediate **H** (Scheme 5), we added a chiral ligand to perform the reaction. The use of (*S*)-DM-SEGPHOS led to an induction of chirality (21% of enantiomeric excess), confirming the presence of the metal during the [3 + 2] cycloaddition step (Scheme 8). In another hand, the use of gold complexes bearing chiral ligands didn't show any chirality induction, suggesting the formation of metal-free nitrone **J** (Scheme 5).

Under these conditions, a mixture of products **9b** and **10b** was obtained; chiral induction was only observed for compound **9b**, suggesting that only its formation was influenced by the metal. The conversion was full, indicating that the reaction did not involve kinetic resolution.

Then, the value of this divergent process catalyzed by either gold or silver could also be established by performing a scale-up and some post-functionalization experiments (Scheme 9). The gram-scale transformation of **5b** was performed on 3 mmol and led to **9b** in 56% and **10b** in 52% yield respectively (Scheme 9, (a)). Rewardingly, compounds **9b** and **10b** were subjected to several post-functionalization reactions to access new and original structures (Scheme 9, (b)). Carboxylic acids compounds **12** and **13** were obtained from respectively **9b** and **10b** using LiOH with both 98% of yields.

The reduction of the ester and the ketone of compound **10b**, using $LiAlH_4$, led to compound **15** in 96% yield. These two modifications greatly enhanced the substrate's capacity to form hydrogen bonds, a characteristic commonly observed in

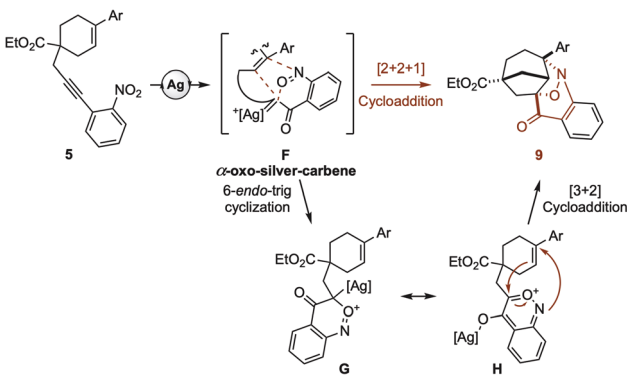

Scheme 7 Formation of **9** *via* a [2 + 2 + 1] cycloaddition.

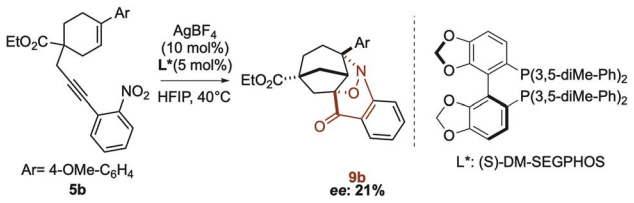

Scheme 8 Formation of **9** *via* a [2 + 2 + 1] cycloaddition.

biologically active molecules.[21] Compound **9b** was also subjected to a non-optimized HWE reaction, leading to the corresponding (*E*)-alkene **14** in 24% yield. Finally, a wide range of bicyclo[3.2.1]octyl amides have shown biological activities, as drugs for central nervous system diseases or anxiety disorders,[22]

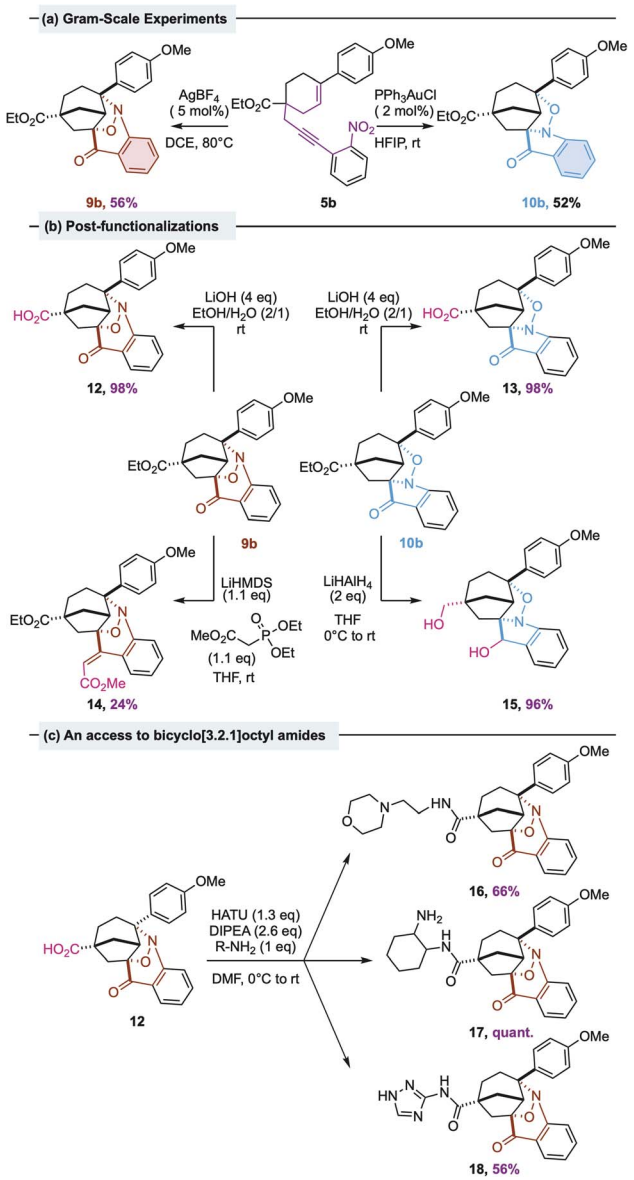

Scheme 9 Gram-scale experiments and post-functionalization reactions.

but also as adenosine receptor antagonists[23] and thus have been patented in the last decade. In this context, we demonstrated that peptidic couplings were efficiently possible starting from compound **12**, to reach three bicyclo[3.2.1]octyl amides in good to quantitative yields (Scheme 9(c), **16**, **17**, **18**).

By using different kind of amines, we can provide an access to a huge number of molecules with potential biological activity. The reaction is completely diastereoselective and occurred under mild conditions.

Conclusion

In summary, we have developed a divergent synthesis of heterohexacyclic derivatives *via* a silver or gold-catalyzed cascade cycloisomerization/[3 + 2] or [2 + 2 + 1] cycloaddition in HFIP. We designed and optimized selective conditions for the formation of two different families of complexes scaffolds, bearing both a bicyclo[3.2.1]octane unit and respectively a benzoxazinone or a pseudoindoxyl moiety. We showed that interactions of HFIP with silver and gold were relevant making HFIP a key player in this study. The starting 1,6-enyne derivatives were conveniently synthesized through efficient, and high-yielding reactions, including two palladium-catalyzed cross-coupling reactions. The core framework of these products was assembled *via* a [3 + 2] or [2 + 2 + 1] cycloaddition involving α-carbonyl carbenoids, nitroso intermediates, and internal alkenes. We showed that depending on the metal, a five-membered or a six-membered ring intermediate was favored, followed by a *N*- or a *O*-cyclization leading to two different hexacyclic derivatives. DFT calculations and control experiments were also carried out to support the proposed mechanism. Finally, we significantly increased the molecular complexity of our scaffolds, by the creation in a single step of 3 stereogenic centers and 3 cycles *via* the formation of C–C, C–O and C–N bonds. These building blocks contain key units commonly found in various biologically active natural products and could also be valued by several post-functionalizations. In a context of enhancing molecular diversity and complexity in chemical libraries, the tridimensional character of our compounds is currently investigated *via* PMI (principal moment of inertia) analysis and will be described in due course.

Author contributions

E. G. and A. B. carried out synthesis, optimization, substrate scope, and mechanistic studies. F. F.-V. performed the DFT calculations. E. G. wrote the first version of the manuscript and SI, all authors then contributed to the full preparation and participated in discussions. V. D., J.-M. F. and V. M. supervised the PhD student E. G. V. M. directed the project. All authors have given approval to the final version of the manuscript.

Conflicts of interest

There are no conflicts to declare.

Data availability

Catalysis in HFIP: Silver- and gold-catalyzed divergent cascade cycloisomerization/[3 + 2] *versus* [2 + 2 + 1] cycloaddition towards a stereoselective access to heterohexacyclic derivatives.

CCDC 2362171 and 2362169 contain the supplementary crystallographic data for this paper.[24]

Supplementary information is available. See DOI: **https://doi.org/10.1039/d5sc05338b**.

Acknowledgements

This work was supported by the Centre National de la Recherche Scientifique (CNRS) and the Université Côte d'Azur. Financial support from the Centre National de la Recherche Scientifique and the Université Côte d'Azur is gratefully acknowledged. We also gratefully acknowledge Institut Servier d'Innovation Thérapeutique for a PhD grant to E.G and for some HRMS and NMR analyses. We are grateful to MS3U-FR2769 platform (Sorbonne Université) for HRMS analyses and to Dr M. Giorgi (Aix-Marseille University) for X-ray analyses of **9b** and **10b**. The authors are grateful to the Université Côte d'Azur's Center for High-Performance Computing (OPAL infrastructure) for providing resources and support.

Notes and references

1 (*a*) F. Lovering, J. Bikker and C. Humblet, *J. Med. Chem.*, 2009, **52**, 6752–6756; (*b*) F. Lovering, *Med. Chem. Commun.*, 2013, **4**, 515; (*c*) J. Meyers, M. Carter, N. Y. Mok and N. Brown, *Future Med. Chem.*, 2016, **8**, 1753–1767.

2 (*a*) N. Asao, K. Sato and Y. Yamamoto, *Tetrahedron Lett.*, 2003, **44**, 5675–5677; (*b*) X. Li, T. Vogel, C. D. Incarvito and R. H. Crabtree, *Organometallics*, 2005, **24**, 62–76.

3 (*a*) P. Patel and C. V. Ramana, *Org. Biomol. Chem.*, 2011, **9**, 7327; (*b*) L. W. Chen, J. L. Xie, H. J. Song, Y. X. Liu, Y. C. Gu and Q. M. Wang, *Org. Chem. Front.*, 2017, **4**, 1731–1735.

4 (*a*) S. Zhou, Q. Liu, M. Bao, J. Huang, J. Wang, W. Hu and X. Xu, *Org. Chem. Front.*, 2021, **8**, 1808–1816; (*b*) G. Chen, Y. Wang, J. Zhao, X. Zhang and X. Fan, *J. Org. Chem.*, 2021, **86**, 14652–14662; (*c*) P. S. Dhote and C. V. Ramana, *Org. Lett.*, 2019, **21**, 6221–6224.

5 A. M. Jadhav, S. Bhunia, H.-Y. Liao and R.-S. Liu, *J. Am. Chem. Soc.*, 2011, **133**, 1769–1771.

6 *Silver in Organic Chemistry*, ed. M. Harmata, Wiley, New Jersey, 2010.

7 (*a*) A. Arcadi, M. Chiarini, L. Del Vecchio, F. Marinelli and V. Michelet, *Eur. J. Org Chem.*, 2017, **2017**, 2214–2222; (*b*) A. Arcadi, M. Chiarini, L. Del Vecchio, F. Marinelli and V. Michelet, *Chem. Commun.*, 2016, **52**, 1458–1461.

8 Selected reviews:(*a*) I. Colomer, A. E. R. Chamberlain, M. B. Haughey and T. J. Donohoe, *Nat. Rev. Chem.*, 2017, **1**, 0088; (*b*) H. F. Motiwala, A. M. Armaly, J. G. Cacioppo, T. C. Coombs, K. R. K. Koehn, V. M. Norwood and J. Aubé, *Chem. Rev.*, 2022, **122**, 12544–12747; (*c*) M. Piejko, J. Moran and D. Lebœuf, *ACS Org. Inorg. Au*, 2024, **4**, 287–300; (*d*)

X.-D. An and J. Xiao, *Chem. Rec.*, 2020, **20**, 142–161; Selected use of HFIP in total synthesis and for its Lewis acid properties:; (*e*) Y.-N. Ma, Y. Gao, Y. Ma, Y. Wang, H. Ren and X. Chen, *J. Am. Chem. Soc.*, 2022, **144**, 8371–8378; (*f*) V. Pozhydaiev, M. Power, V. Gandon, J. Moran and D. Lebœuf, *Chem. Commun.*, 2020, **56**, 11548–11564; (*g*) M. Van Hoof, R. J. Mayer, J. Moran and D. Lebœuf, *Angew. Chem., Int. Ed.*, 2024, e202417089; (*h*) S. Deswal, R. Chandra Das, D. Sarkar and A. T. Biju, *Angew. Chem., Int. Ed.*, 2025, e202501655.

9 Au:(*a*) N. V. Tzouras, L. P. Zorba, E. Kaplanai, N. Tsoureas, D. J. Nelson, S. P. Nolan and G. C. Vougioukalakis, *ACS Catal.*, 2023, **13**, 8845–8860; (*b*) N. V Tzouras, A. Gobbo, N. B. Pozsoni, S. G. Chalkidis, S. Bhandary, K. Van Hecke, G. C. Vougioukalakis and S. P. Nolan, *Chem. Commun.*, 2022, **58**, 8516–8519; (*c*) A. Truchon, A. Dupeux, S. Olivero and V. Michelet, *Adv. Synth. Catal.*, 2023, **365**, 2006–2012; Fe:; (*d*) V. Pozhydaiev, A. Paparesta, J. Moran and D. Lebœuf, *Angew. Chem., Int. Ed.*, 2024, e202411992; Au/Ru:; (*e*) C. Xu, Y. Feng, F. Li, J. Han, Y.-M. He and Q.-H. Fan, *Organometallics*, 2019, **38**, 3979–3990; Pd:; (*f*) T. Bhattacharya, A. Ghosh and D. Maiti, *Chem. Sci.*, 2021, **12**, 3857–3870.

10 (*a*) E. Kaplanai, N. V. Tzouras, N. Tsoureas, N. B. Pozsoni, S. Bhandary, K. Van Hecke, S. P. Nolan and G. C. Vougioukalakis, *Dalton Trans.*, 2024, **53**, 11001–11008; (*b*) W. Wang, X. Cao, W. Xiao, X. Shi, X. Zuo, L. Liu, W. Chang and J. Li, *J. Org. Chem.*, 2020, **85**, 7045–7059.

11 (*a*) V. Davenel, C. Nisole, F. Fontaine-Vive, J.-M. Fourquez, A.-M. Chollet and V. Michelet, *J. Org. Chem.*, 2020, **85**, 12657–12669; (*b*) V. Davenel, C. Puteaux, C. Nisole, F. Fontaine-Vive, J.-M. Fourquez and V. Michelet, *Catalysts*, 2021, **11**, 546–550; (*c*) A. Truchon, A. Dupeux, S. Olivero and V. Michelet, *Org. Chem. Front.*, 2024, **11**, 4070–4076; (*d*) Y. Tang, I. Benaissa, M. Huynh, L. Vendier, N. Lugan, S. Bastin, P. Belmont, V. César and V. Michelet, *Angew. Chem., Int. Ed.*, 2019, **58**, 7977–7981; (*e*) A. Truchon, M. Gorodnichy, S. Olivero and V. Michelet, *Org. Lett.*, 2024, **26**, 6698–6702.

12 M. Barp, F. Kreuter, H. Buttkus, J. Jin, M. Kretzschmar, R. Tonner-Zech, K. Asmis and T. Gulder, *Angew. Chem., Int. Ed.*, 2025, **64**, e202417889.

13 Selected reviews: (*a*) L. Li, Z. Chen, X. Zhang and Y. Jia, *Chem. Rev.*, 2018, **118**, 3752–3832; (*b*) Y. Wang, J. Feng, E.-Q. Li, Z. Jia and T.-P. Loh, *Org. Biomol. Chem.*, 2024, **22**, 37–54; (*c*) C. C. Chintawar, A. K. Yadav, A. Kumar, S. P. Sancheti and N. T. Patil, *Chem. Rev.*, 2021, **121**, 8478–8558.

14 A. Carrër, C. Péan, F. Perron-Sierra, O. Mirguet and V. Michelet, *Adv. Synth. Catal.*, 2016, **358**, 1540–1545.

15 B. Scheiper, M. Bonnekessel, H. Krause and A. Fürstner, *J. Org. Chem.*, 2004, **69**, 3943–3949.

16 P. S. Dhote, S. V. Halnor and C. V. Ramana, *Chem. Rec.*, 2021, **21**, 3546–3558.

17 CCDC2362171 (**9b**) and CCDC2362169 (**10b**) contains the supplementary crystallographic data for this paper. For details, see the SI.

18 Following referee inquiries, we conducted the reactions in the presence of ditertbutylpyridine and triphenylphosphine oxide instead of triphenylphosphine, as well as in the presence of 5 equivalents of water in HFIP but no conversion was observed.

19 Relative free energies of intermediates I and G in presence of $AgBF_4$ or PPh_3AuCl as catalysts with respect to the most stable. Values are in kcal/mol. For details, see the SI.

20 The reaction of **11** in the presence of gold or silver catalyst led to no conversion. Considering its formation, we therefore cannot exclude that the reaction could proceed *via* a three-membered ring intermediate.

21 C. Bissantz, M. Kuhn and M. Stahl, *J. Med. Chem.*, 2010, **53**, 5061–5084.

22 W. F. Kiesman, J. E. Dowling, C. L. Ensinger, G. Kumaravel, R. C. Petter, K. C. Lin and H. X. Chang, Biogen Inc., *EP1230243*, 2002.

23 G. Li, H. Zhou, J. Weiss, D. Doller and J. H. Ford, Lundbeck, *WO2012088365A1*, 2012.

24 E. Gentilini, A. Bouschon, V. Davenel, F. Fontaine-Vive, J.-M. Fourquez and V. Michelet, *CCDC 2362171: Experimental Crystal Structure Determination*, 2025, DOI: **10.5517/ccdc.csd.cc2k9120**; E. Gentilini, A. Bouschon, V. Davenel, F. Fontaine-Vive, J.-M. Fourquez and V. Michelet, *CCDC 2362169: Experimental Crystal Structure Determination*, 2025, DOI: **10.5517/ccdc.csd.cc2k910y**.